

Supporting Information

Abnormal spectral broadening of ordered structure near-infrared phosphor $\text{La}_2\text{CaHfO}_6:\text{Cr}^{3+}$

*Yulei Zhao^a, Xudong Wang^a, Qihao Wang^a, Tianliang Zhou^{a, *}, Yousan Chen^b,*

*Jianxing Xu^b, Xueyuan Tang^{a, *}, Rong-Jun Xie^{a, c, *}*

^a Fujian Province Key Laboratory of Surface and Interface Engineering for High-Performance Materials, and Xiamen University, Xiamen 361005, China

^b Xiamen Leedarson Digital Education Technology Co. Ltd., Xiamen 361015, China

^c State Key Laboratory of Physical Chemistry of Solid Surfaces, Xiamen University, Xiamen 361005, China

Corresponding Authors

*Email: bible2@163.com (T.Z.).

*Email: xytang@xmu.edu.cn (X.T.)

*Email: rjxie@xmu.edu.cn (R.-J. X.)

Table S1 Crystallographic data of LCH:0.02Cr³⁺.

Atom	x	y	z	Occupancy
La1	0.5107	0.4496	0.24908	1.01297
Ca1	0.5	0	0	0.58011
Cr1	0.5	0	0	0.00483
Hf1	0	0.5	0	0.48466
Cr1	0	0.5	0	0.00467
O1	0.2982	0.3294	0.94264	0.98372
O2	0.3625	0.0439	0.26427	1.21869
O3	0.1807	0.7889	0.93318	1.18128

The result is obtained by the Rietveld refinement, the analysis is carried out under the double position occupancy.

The crystal-field parameters were calculated by the following equations

$$10D_q = E(^4T_2) - E(^4A_2 \rightarrow ^4T_2) - \Delta S/2 \quad (1)$$

$$\frac{Dq}{B} = \frac{15 * \left(\frac{\Delta E}{Dq} - 8\right)}{\left(\frac{\Delta E}{Dq}\right)^2 - 10 \left(\frac{\Delta E}{Dq}\right)} \quad (2)$$

$$\Delta E = E(^4T_1) - E(^4T_2) = E(^4A_2 \rightarrow ^4T_1) - E(^4A_2 \rightarrow ^4T_2) \quad (3)$$

Where Dq denotes the crystal field parameter, B is the Racah parameter, the E(⁴T₁) and E(⁴T₂) represent the energy level positions of ⁴T₁ and ⁴T₂, respectively.

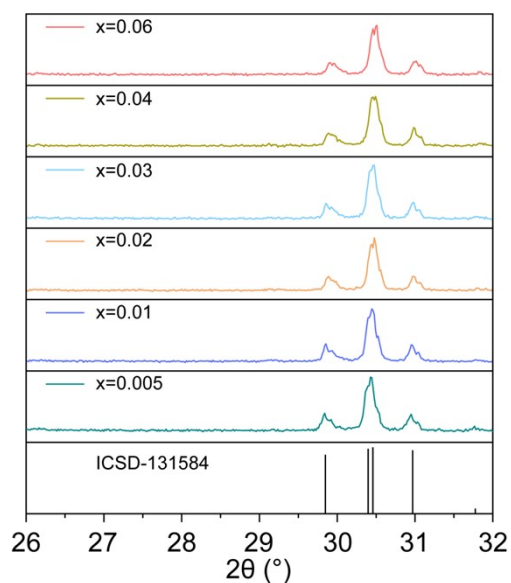


Fig. S1. Enlarged LCH:xCr³⁺ ($x = 0-0.06$) XRD patterns of the portion, showing the diffraction peak shift.

With the adding of Cr³⁺, the XRD peaks of LCH:xCr³⁺ sample shows a slightly move to the large angle, which is caused by the radius difference between Ca²⁺, Hf⁴⁺ and Cr³⁺.

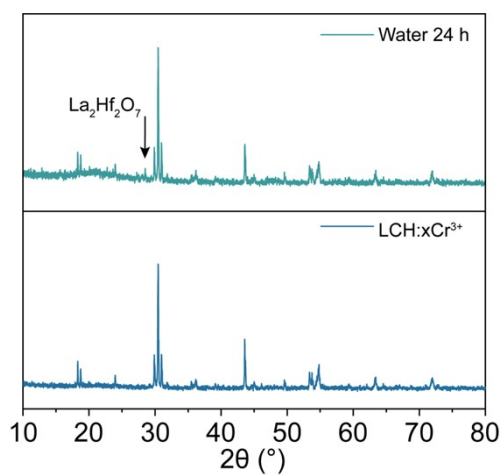


Fig. S2. XRD comparison between the original sample and the samples soaked for 24 h.

After soaking in water for 24 h, the XRD pattern of LCH:0.02Cr³⁺ sample shows a clearly peak, which belongs to La₂Hf₂O₇.

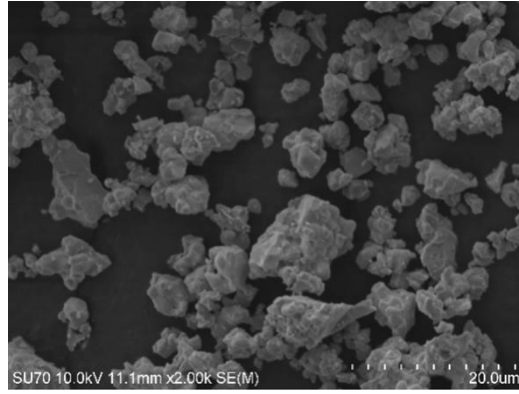


Fig. S3. Size distribution of $\text{La}_2\text{CaHfO}_6:0.02\text{Cr}^{3+}$.

Samples of different particle sizes can be seen from this picture, and no obvious morphological changes caused by doping have been observed.

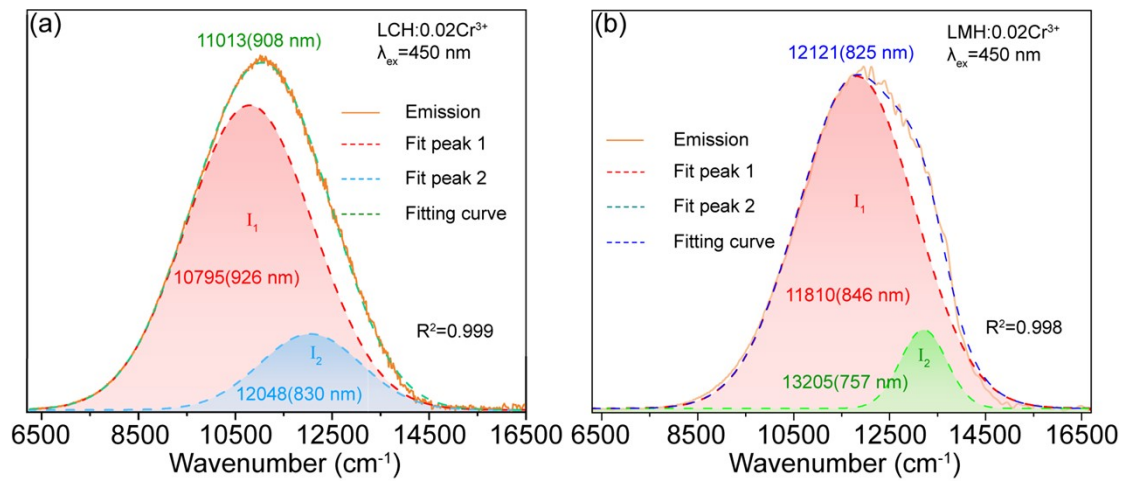


Fig. S4. The Gaussian fitting of PL of (a) LCH:0.02Cr³⁺ and (b) LMH:0.02Cr³⁺.

The emission peak of LCH is located at 908 nm, and the two Gaussian peaks centered at 830 nm and 926 nm, respectively. The PL peak of LMH is located at 825 nm, and the two Gaussian peaks centered at 757 nm and 846 nm, respectively.

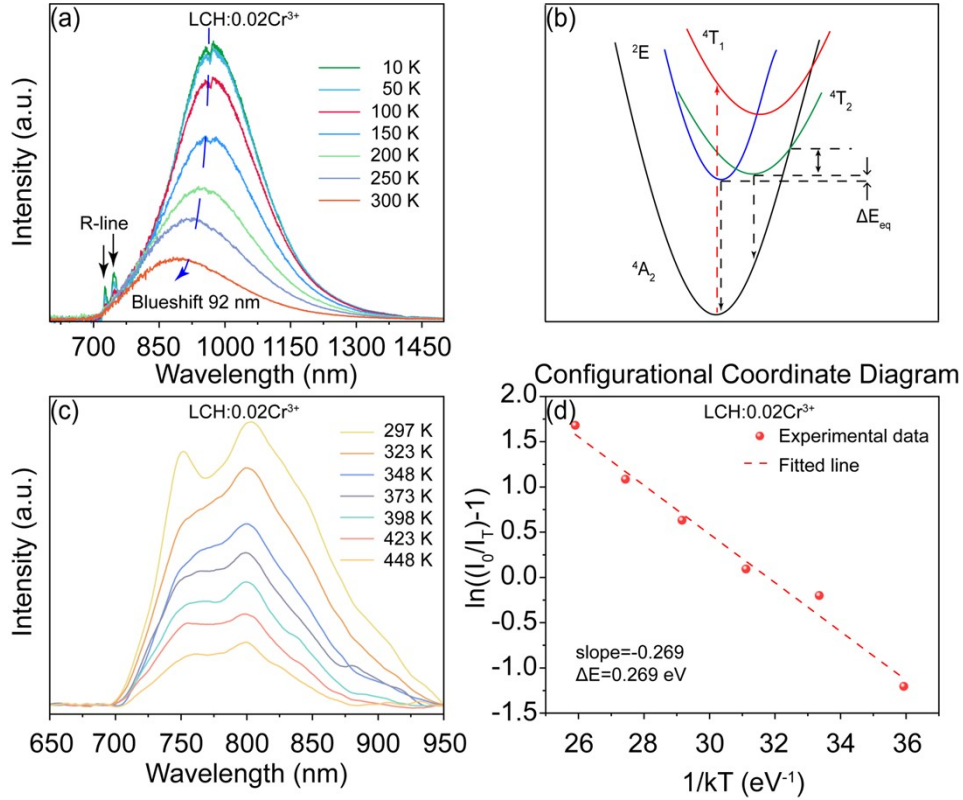


Fig. S5. (a) Temperature-dependent PL of LCH:0.02Cr³⁺ under 450 nm excitation in range of 10-300K, (b) Configurational coordinate diagram of LCH:0.02Cr³⁺, (c) Temperature-dependent PL of LCH:0.02Cr³⁺ under 450 nm excitation in range of 300-448K, (d) The relationship graph between $\ln(I_0/I_x)-1$ and $\log x$.

The emission peak of spectra show an obviously blue shift while the temperature change from 10 K to 300 K, and R-line disappear with the increase of temperature. According to Temperature-dependent PL of 300 K-448 K, the thermal quenching activation energy (ΔE) is calculated to be 0.269 eV.

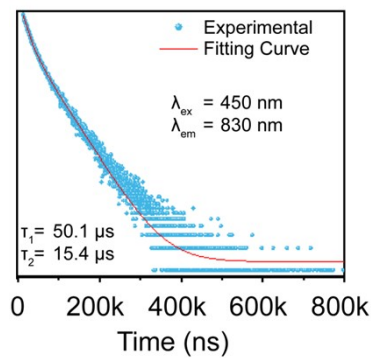


Fig. S6. Decay time of LCH:0.02Cr³⁺ monitoring at 830 nm.

All the samples share the same tendency with the change of monitoring wavelength. The energy

transfer between different sites, which can be replaced by Cr³⁺ is verified.

The decay time is calculated by the following bio-exponential function

$$I(t) = I_0 + \sum_{i=1}^n A_i \exp\left(-\frac{t}{\tau_i}\right) \quad (4)$$

$I(t)$ represents luminescent intensity at time t , I_0 and A_i are fitting constants.

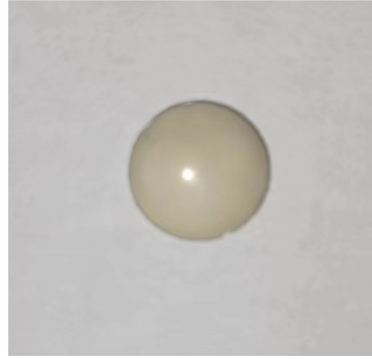


Fig. S7. The NIR lighting source.

The length of the fiber is 2 m, and the diameter is 5 mm, which the diameter of the inner part is 4 mm. Therefore, the valid area of cable is 12.57 mm². The emission peak of the LED is 450 nm, and the diameter and thickness of the NIR light is 10 mm and 1.4 mm. The input power of power source is 0.063 mW, and the output power is 0.0016 mW. The results of the transmittance of blue and NIR lights is 0.819 and 0.91, respectively. Considering the input power, the insertion loss (IL) is 15.95 based on the equation $IL = -10 \lg(P_{out}/P_{in})$.

The tolerance factor is an extremely important parameter for perovskite materials. and can be calculated by the following equation,

$$t = \frac{(R_A + R'_A)/2 + R_O}{\sqrt{2}[(R_B + R'_B)/2 + R_O]} \quad (5)$$

Generally tolerance factor is a measure of distortion which occurs in a sample when doped element enters into the sample. It also represents the presence of ferroelectricity with in a sample. Variation of tolerance factor affected by the substitution of dopants in ABO₃ lattice and also it influences the structural phase transitions in a sample are tailored from relaxor to normal and vice versa¹. After literature reading and research, we found that for double perovskite NIR materials, when the tolerance factor is in the middle of the range, it often presents a standard NIR emission, and the deviation is relatively small. When the tolerance factor is too large or too small, its luminescence

often has a large deviation. Therefore, we believe that there is a relationship between tolerance factor and FWHM. Based on this, we started our research. The above content has been added to the supporting information.

1. C. S. Devi, J. Omprakash, A. R. Malathi, G. S. Kumar and G. Prasad, *Ferroelectrics*, 2020, **554**, 172-186.